Supplementary materials for

Highly sensitive benzothiazole-based chemosensors for detection and bioimaging of peroxynitrite in living cells

Yaqiong Kong[a], Rong Wu[a], Xiaodong Wang[a], Guoxu Qin[a], Fengyi Wu[a], Chunyu Wang[a,c], Minmin Chen[a], Nannan Wang[a,*], Qian Wang[b,*], Duojun Cao[a,*]

[a]Engineering Technology Center of Department of Education of Anhui Province, Institute of Novel Functional Materials and Fine Chemicals, and College of Chemistry and Materials Engineering, Chaohu University, Chaohu 238024, PR China

[b]Department of Radiation Oncology, China-Japan Union Hospital of Jilin University, Changchun 130000, PR China

[c]School of Information Science and Technology, University of Science and Technology of China, Hefei, Anhui 230026, China

*E-mail: 053076@chu.edu.cn (Duojun Cao), wangqian1991@jlu.edu.cn (Qian Wang), nnw1990@126.com (Nannan Wang)

EXPERIMENTAL SECTION

Materials and Instruments

Unless otherwise mentioned, all reagents were purchased commercially and used without further purification. Deionized water was used throughout all experiments. 10 mM stocking solution of **BS1 and BS2** were prepared in DMSO and conserved under -18 ^{o}C for later use. All the fresh active species were prepared according to the previous literature. And the other solutions of analytes were prepared in deionized water. Besides, the working solutions were achieved by diluting with PBS solution (10 mM, containing 25% DMSO, pH = 7.4). Accurate pH values of the solutions were adjusted by slight amount of NaOH or HCl (1 M). The UV-vis spectra were recorded on a Beijing Purkinje T9CS UV-vis spectrophotometer and fluorescent spectra were recorded using a F97XP fluorescence spectrophotometer with a 10 mm quartz cuvette and slit widths of 5 nm. ^{1}H NMR data were collected on the Bruker Avance NMR spectrometer (400 MHz). FTIR analysis was recorded on the FTIR-650 (Tianjin Gangdong SCI&Tech). The reverse-phase HPLC was recorded in the Waters ACQUITY UPLC H-Class PLUS (70% methanol in water). Electrospray ionization (ESI) mass spectrometric data were acquired on a Thermo UPLC-Q Exactive Orbitrap HR-MS spectrometer. pH measurements were conducted on a Model PHS-3CT pH-meter. Fluorescent confocal imaging was operated with a Zeiss LSM 710 microscope and the quantitative fluorescence intensity was analyzed via Image J program.

Synthesis and Characterization of BS1 and BS2

The synthesis routes of **BS1** and **BS2** were outlined in Scheme 1. Two benzaldehydes **1** and **2** were synthesized according to the previous literatures [1, 2].

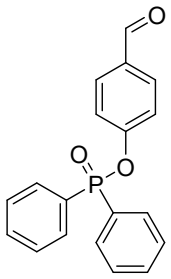

1

Synthesis of benzaldehyde **1:** 4-Hydroxybenzaldehyde (244 mg, 2 mmol) was added into a solution of Et_3N (280 μL, 2 mmol) in THF (25 mL) at 0 °C and stirred for 20 min. Subsequently, to the above mixture was added diphenylphosphinic chloride (320 μL, 1.6 mmol) dropwise and stirred at room temperature for 2 h. when the original materials consumed, the organic solvent was removed under vacuum and purified by the flash chromatography eluted by EtOAc/PE to obtained compound **1** as a faint yellow solid (390 mg, 75%). ^{1}H NMR (400 MHz, $CDCl_3$, δ ppm) 9.91 (s, 1H), 7.94-7.88 (m, 4H), 7.80 (d, J = 8.0 Hz, 2H), 7.57 (t, J = 4.0 Hz, 2H), 7.52-7.47 (m, 4H), 7.41 (d, J = 12.0 Hz, 2H).

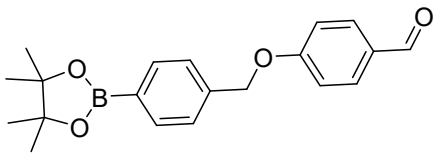

2

Synthesis of benzaldehyde **2:** 4-hydroxybenzaldehyde (268.4 mg, 2.2 mmol) and 4-Bromomethylphenylboronic acid pinacol ester (594 mg, 2.0 mmol) were firstly dissolved in dry DMF (10 mL), following by adding anhydrous K_2CO_3 (300 mg, 2.2 mmol). And the mixture stirred at 120 °C for 6 h. After cooling to room temperature, the solution was poured into deionized water and extracted by dichloromethane. The organic layer was collected, dried over anhydrous sodium sulfate, and concentrated. The crude product was purified by flash chromatography eluted by EtOAc/PE to afford **2** as a white solid. (485 mg, 72%). ^{1}H NMR (400 MHz, $CDCl_3$, δ ppm) 9.90 (s, 1H), 7.86 (t, J = 8.0 Hz, 4H), 7.45 (d, J = 8.0 Hz, 2H), 7.09 (d, J = 8.0 Hz, 2H), 5.20 (s, 2H), 1.37 (s, 12H).

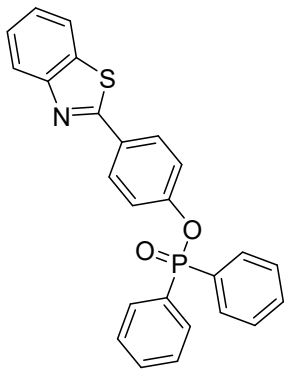

BS1

Synthesis of probe **BS1**: Primarily, compound **1** (322 mg, 1.0 mmol) and 2-aminobenzenethiol (125 mg, 1.0 mmol) were dissolved in anhydrous ethanol (10 mL) and then a catalytic amount of $La(NO_3)_3 \bullet 6H_2O$ was added into the solution. The reaction mixture was stirred for 2 h and a white solid precipitated. The crude product was obtained by filtration and purified by flash chromatography (EtOAc/PE) to afford white **BS1** solid (370 mg, 86%).^{1}H NMR (400 MHz, $CDCl_3$, δ ppm) 8.05 (d, J = 8.0 Hz, 1H), 8.00 (d, J = 8.0 Hz, 2H), 7.96 (s, 1H), 7.94 (dd, J_1 = 8.0 Hz, J_2 = 8.0 Hz, 2H), 7.91 (t, J = 8.0, 2H), 7.61-7.57 (m, 2H), 7.53-7.48 (m, 5H), 7.39 (t, J = 8.0, 3H). ^{13}C NMR (400 MHz, $CDCl_3$, δ ppm): 166.96, 154.10, 153.21, 153.13, 135.05, 132.72, 132.69, 131.87, 131.77, 131.25, 130.15, 129.88, 129.08, 128.80, 128.67, 126.36, 125.19, 125.14, 123.14, 121.62, 121.33, 121.28. HR-MS (ESI): m/z calcd for $C_{25}H_{18}NO_2PS$: 427.0796, found $[M + H]^+$ 428.0898.

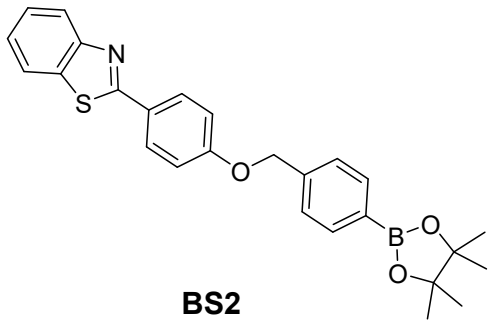

BS2

Synthesis of probe **BS2**: Probe **BS2** was obtained as a white solid in a similar method as **BS1** in the yield of 82%. ^{1}H NMR (400 MHz, $CDCl_3$, δ ppm) 8.11 (d, J = 8.0 Hz, 1H), 7.94 (d, J = 12.0 Hz, 1H), 7.55-7.43 (m, 4H), 7.41 (d, J = 8.0 Hz, 4H), 7.09 (d, J = 8.0 Hz, 2H), 5.20 (s, 2H), 1.37 (s, 12H). HR-MS (ESI): m/z calcd for $C_{26}H_{26}BNO_3S$: 443.1726, found $[M + H]^+$ 444.1824.

Determination of fluorescence quantum yield (Φ_F)

The quantum yield of **BS1** or **BS2** with and without $ONOO^-$ was measured with anthracene in ethanol solution as standard (Φ_F =0.27) [3]. The absorbance of these solutions should be below 0.05 to minimize the effect of re-absorption. And the excitation wavelength was set at 365 nm with the emission wavelength ranging from 385-600 nm (slit widths: 5 nm). The final quantum yields were calculated based on the following equation [4]:

$$\Phi_{F(x)}=\Phi_{F(s)}\times(A_sF_x/A_xF_s)\times(n_x/n_s)^2$$

A_S and A_X refer to the absorbance at the excitation of the standard and the samples (A<0.05), respectively. F_S and F_X were the areas under the corrected emission curve of fluorescence standard and samples. n_S and n_X were the refractive indexes of the solvents dissolving fluorescence standard and samples. Finally, $\Phi_{F(S)}$ and $\Phi_{F(X)}$ refer to the fluorescence quantum yield of standard and testing samples.

General procedure for spectroscopic studies

A stock solution of probe (10 mM) was prepared in DMSO. Peroxynitrite ($ONOO^-$) solution was prepared following the reported literature [5]. Briefly, a mixture of sodium nitrite (0.6 M) and hydrogen peroxide (0.7 M) was acidified with hydrochloric acid (0.6 M), and sodium hydroxide (1.5 M) was added within 1-2s to make the solution alkaline. The concentration of $ONOO^-$ was estimated by using an extinction coefficient of 1670 $M^{-1}cm^{-1}$ at 302 nm. $C_{ONOO^-} = Abs_{302\ nm}$ /1.67 (mM). Singlet oxygen solution ($^1O_2$) was generated in situ by addition 1.0 equiv. of the H_2O_2 stock solution into a solution containing 10.0 equiv. of HClO. Hydroxyl radicals (•OH) was generated by Fenton reaction, $FeCl_2$ was added in the presence of 10.0 equiv. of H_2O_2. Superoxide solution ($O_2^{\bullet -}$) was prepared by adding KO_2 into dry DMSO (DMSO) by stirring vigorously for 10 min. Nitroxyl solution (HNO) was prepared by dissolving Angeli's salt ($Na_2N_2O_3$, AS, the HNO source) in 0.01 M NaOH solution. Nitric oxide (NO) was generated from sodium nitroprusside. Hydrogen peroxide (H_2O_2), hypochlorite (ClO^-) and tert-butyl hydroperoxide (TBHP) were originated from 30%, 70% and 10% aqueous solutions, respectively. The solutions of other test species

were prepared from $ZnCl_2$、$FeCl_3$、NaCl、KNO_3、$Mg(NO_3)_2$、$CuSO_4$、$CaCl_2$、$Al_2(SO_4)_3$、Na_2CO_3、$NaHCO_3$、Na_2SO_3、Na_2SO_4、Na_3PO_4、$NaNO_2$、$NaNO_3$、Vitamin C、Na_2S、AcOK、Cys and GSH in twice-distilled water. Unless otherwise mentioned, all the spectra measurements were conducted in 10 mM PBS-DMSO (3:1, v/v) buffer with pH 7.4. For typical optical measurements, **BS1** or **BS2** was diluted to 10 μM and recorded upon addition of $ONOO^-$ at 298 K by UV-Vis or fluorescence spectra. Emission spectra of the probe in the presence of various biologically relevant species (Na^+、K^+、Fe^{3+}、Zn^{2+}、Cu^{2+}、Ca^{2+}、Al^{3+}、Mg^{2+}、SO_3^{2-}、SO_4^{2-}、CO_3^{2-}、HCO_3^-、NO_2^-、NO_3^-、PO_4^{3-}、Cl^-、H_2S、GSH、Cys、Vitamin C、AcOK、$\cdot OH$、H_2O_2、$^1O_2$、NaClO、NO、TBHP、HNO、$O_2^{\bullet-}$、$ONOO^-$) were measured with excitation at 365 nm.

The limit of detection (LOD) of BS1 and BS2

The emission spectrum of free probe in 10 mM PBS buffer containing 25% DMSO at pH 7.4 was collected for 20 times to confirm the background noise σ [6]. To obtain the slope of the curve (k), the linear regression curve was then fitted according to the data in the range of $ONOO^-$ from 0 to 4.0 μM for **BS1**, and from 0 to 5.0 μM for **BS2**. Then the detection limit was determined from the following equation:

$$\text{Detection limit} = 3\sigma/k$$

Reaction Mechanism

The reaction mechanism has been confirmed by the structural characterization of the reaction product. **BS1**/**BS2** was treated with $ONOO^-$ aqueous solution for 10 min at room temperature. The final reaction mixture was analyzed with HR-MS. And also, to further verify the mechanism, the residue was purified by reverse flash chromatography to record the ^1H NMR, HPLC or FTIR of **BS1** and **BS2** upon addition of $ONOO^-$. The DFT calculation were performed on Gaussian 16 program [7], carried out by Multiwfn 3.8 program [8] and rendered by VMD 1.9.3 program [9].

Cell culture

HepG-2 cells were cultured in DMEM (Dulbecco's modified Eagle's medium, Gibco BRL) medium, which contained 10% FBS (fetal bovine serum, Gibco BRL), 100

μg/mL streptomycin, and 100U/mL penicillin (Gibco BRL). The cells were cultured in a humidified incubator, which provided an atmosphere of 5% CO_2 and 95% air at a constant temperature of 37 °C.

CCK-8 assay

HepG2 cells in the logarithmic phase were harvested and seeded in 96-well plates (5000 cells/well) for 24 h before detection. Then the medium was changed and the experimental group cells were treated with various concentrations (0, 20, 40, 60, 80, 100 μM) of the probe **BS1** for 24 and 48 h, respectively. After that, CCK-8 solution was added to each well, and the plates were incubated for an additional 4 h. The culture medium containing CCK-8 was carefully removed and DMSO was added to each well. Finally, the absorbance at 450 nm was measured by a microplate reader (Infinite M200, Tecan, Männedorf, Switzerland).

Exogenous $ONOO^-$ imaging studies in living HepG2 cells

Before the imaging experiment, HepG-2 cells were seeded on 35 mm glass-bottomed dishes for 24 h. Then the culture medium was removed and the cells were pretreated with SIN-1 (200 μM) in fresh culture medium for 1 h at 37 °C followed by incubated with 10 μM **BS1** for another 30 min at 37 °C. Control for the cells were only incubated with **BS1** under the same condition. Cells were washed with PBS for three times and immediately by confocal fluorescent microscopy with an excitation filter of 405 nm and the collection wavelength range is from 420-490 nm.

Fluorescence imaging of APAP-induced cell damage

HepG-2 cells were pretreated with APAP (0, 100, 250, 500 μM) for 8 h at 37 °C. Then the cells were further incubation with **BS1** (10 μM) for another 30 min at 37 °C. Finally, cell imaging was performed after washing with PBS for three times.

Hepatotoxicity repair in cells

HepG-2 cells were pretreated with GSH (500 μM) for 1 h at 37 °C, followed by incubated with APAP (500 μM) for 8 h and then treated with **BS1** (10 μM) for 30 min. Finally, cell imaging was carried out after washing with PBS for three times.

Table S1 Comparison of fluorescent probes for $ONOO^-$

Structure of probes	Detection limit (M)	Media	Response time	Living cells	Ref.
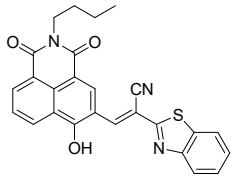	37×10^{-9}	Ethanol/ PBS (5:5)	No	HeLa cells	Ref.[10]
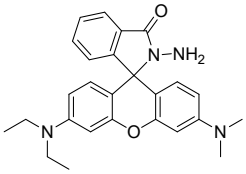	45×10^{-9}	PBS	No	HeLa and RAW 264.7 cells	Ref.[11]
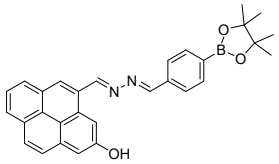	3.54×10^{-6}	DMSO/ PBS (7:3)	No	MCF-7 cells	Ref.[12]
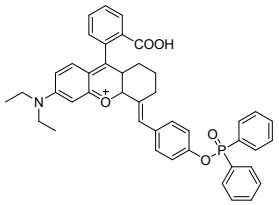	0.4×10^{-6}	DMSO/ PBS (1:1)	No	RAW 264.7 cells	Ref.[13]
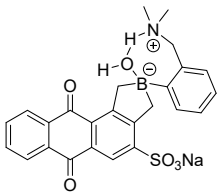	5.4×10^{-6}	52.1%MeOH/ PBS	No	--	Ref.[14]
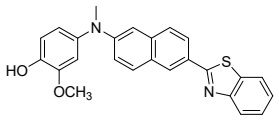	3.5×10^{-8}	1%DMF/ PBS	(<1 min)	RAW 264.7 cells	Ref.[15]
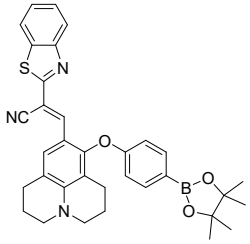	2.5×10^{-6}	10%EtOH / PBS	30 min	J774A.1 cells	Ref.[16]

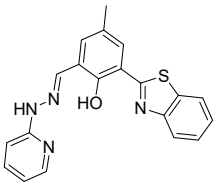	5.8×10^{-8}	5%DMF/ PBS	about 60 s	HeLa cells	Ref.[17]
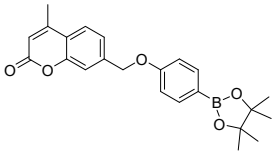	29.8×10^{-9}	1%DMSO /HEPES	5 min	RAW 264.7 cells	Ref.[18]
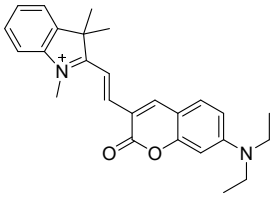	49.7×10^{-9}	PBS	10 min	RAW 264.7 cells	Ref.[19]
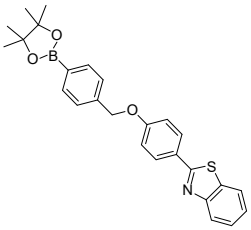	25.2×10^{-9}	25% DMSO /PBS	300 s	--	**This work**
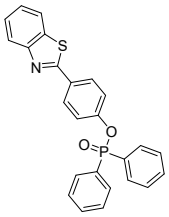	12.8×10^{-9}	25% DMSO /PBS	300 s	HepG2 cells	**This work**

Table S2 The optical properties of the **BS1** and **BS2** in the absence and presence of $ONOO^-$

Compound	λ_{abs} / nm	ε_{max} / M^{-1} cm^{-1}	λ_{em} / nm	δ^a / cm^{-1}	Φ_F
BS1	305	2.58×10^4	--	--	0.05%
BS1 + $ONOO^-$	356	9.98×10^4	430	4834	48.9%
BS2	300	2.92×10^4	--	--	0.03%
BS2 + $ONOO^-$	356	9.36×10^4	430	4834	42.7%
[a]δ is the Stokes shift.					

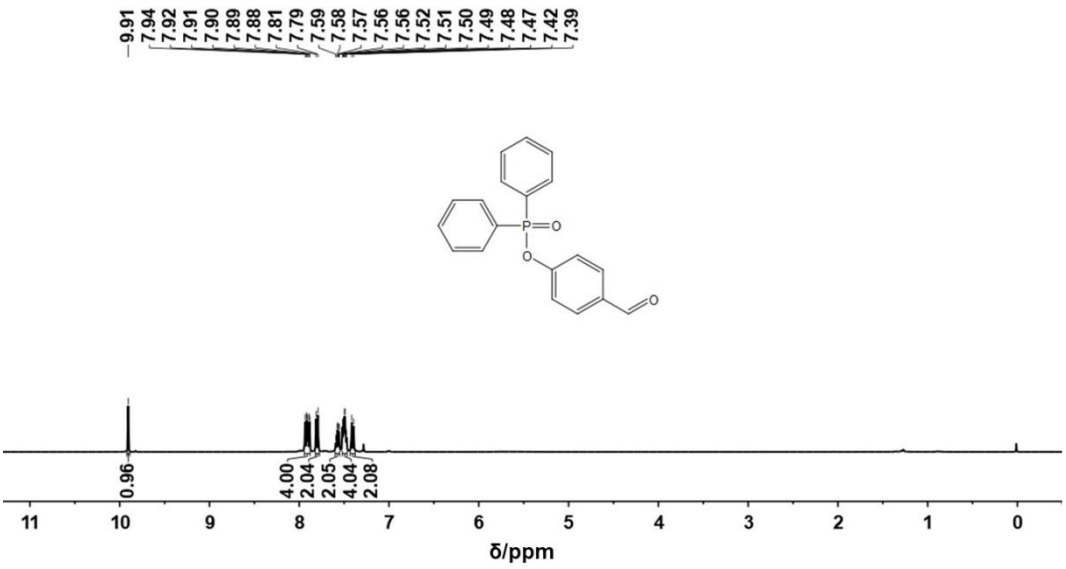

Fig. S1 ^{1}H NMR spectra of benzaldehyde **1** at 298 K (400 MHz) in $CDCl_3$.

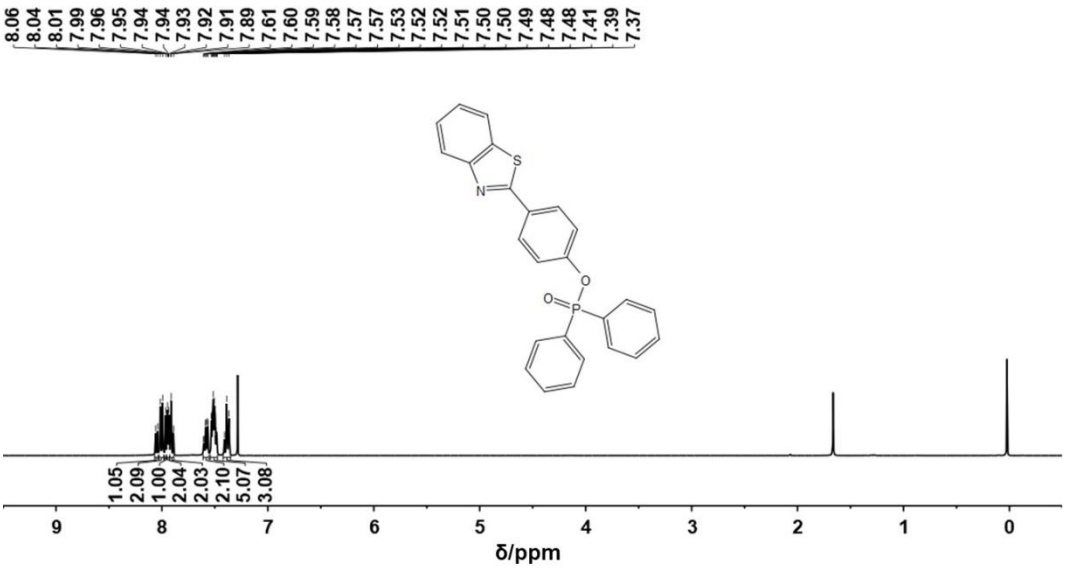

Fig. S2 ^{1}H NMR spectra of probe **BS1** at 298 K (400 MHz) in $CDCl_3$.

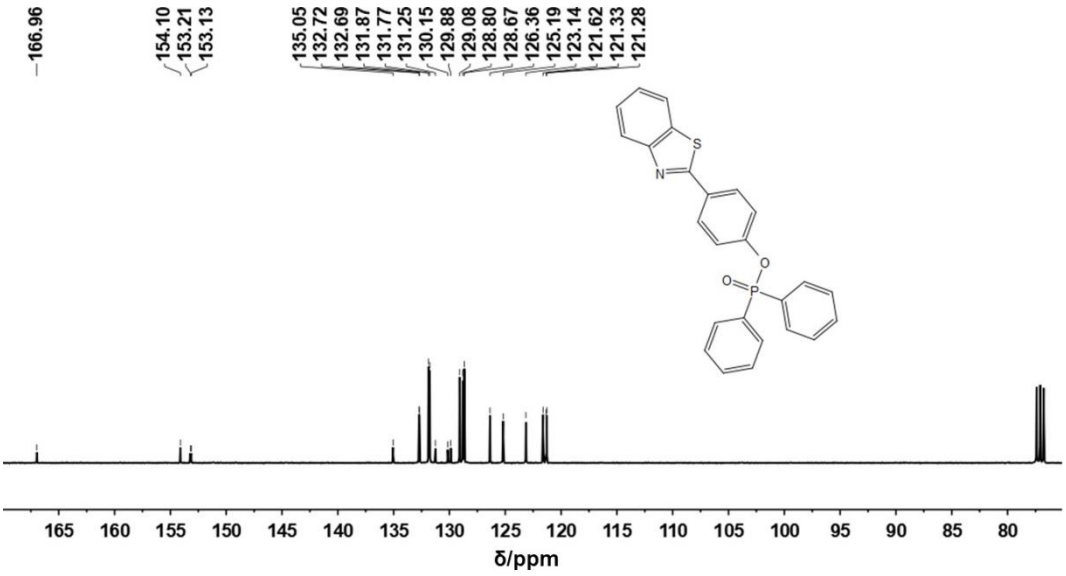

Fig. S3 ^{13}C NMR spectra of probe **BS1** at 298 K (400 MHz) in $CDCl_3$.

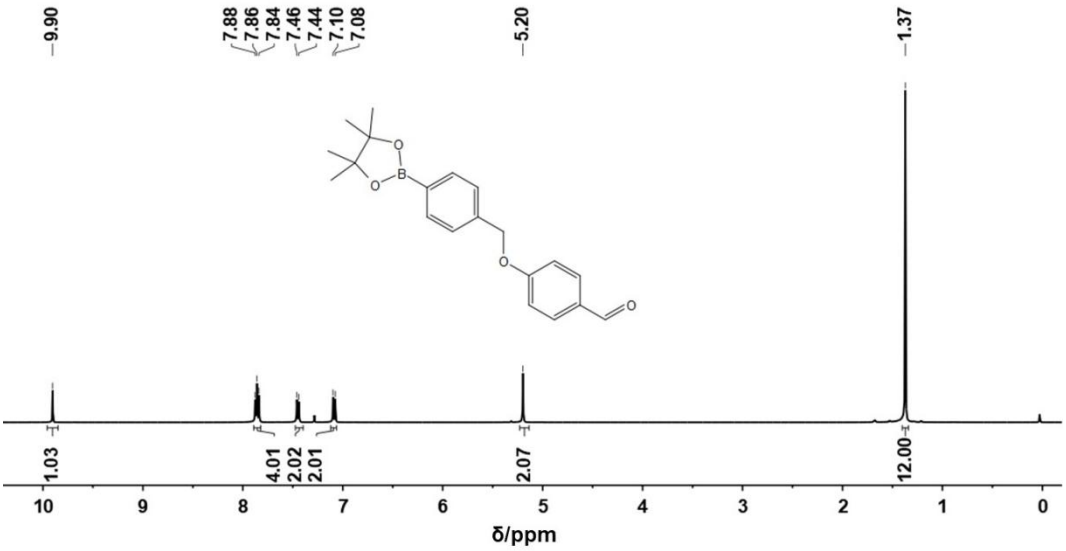

Fig. S4 ^{1}H NMR spectra of benzaldehyde **2** at 298 K (400 MHz) in $CDCl_3$.

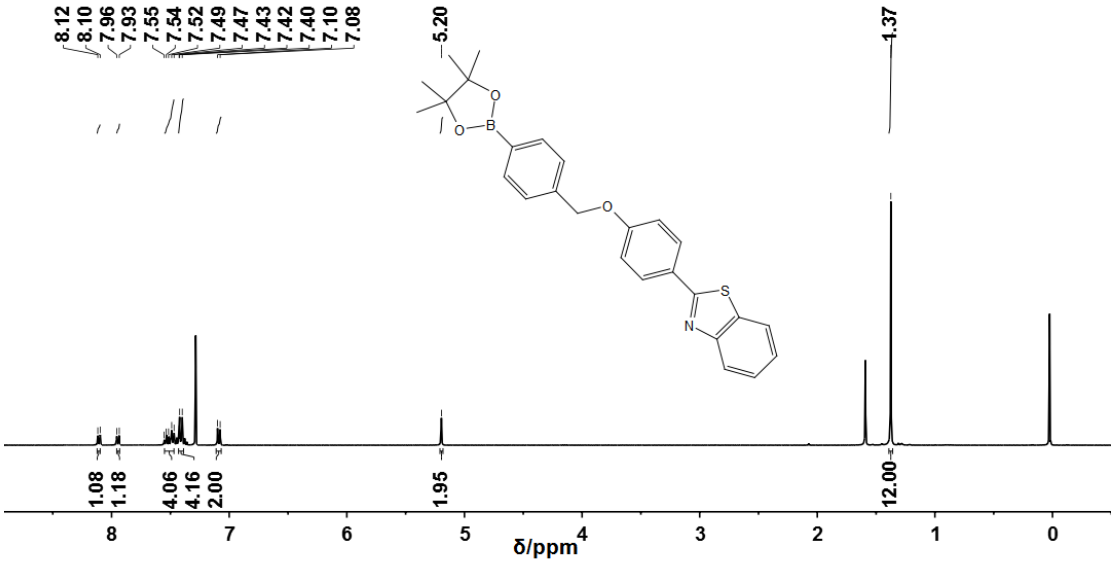

Fig. S5 ^{1}H NMR spectra of probe **BS2** at 298 K (400 MHz) in $CDCl_3$.

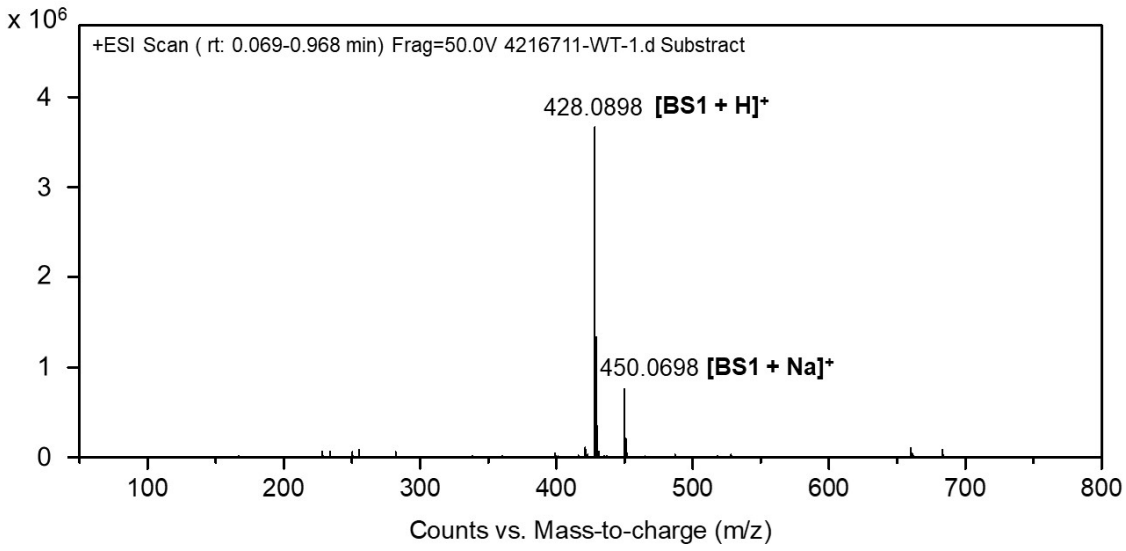

Fig. S6 ESI-high resolution mass spectra of probe **BS1**.

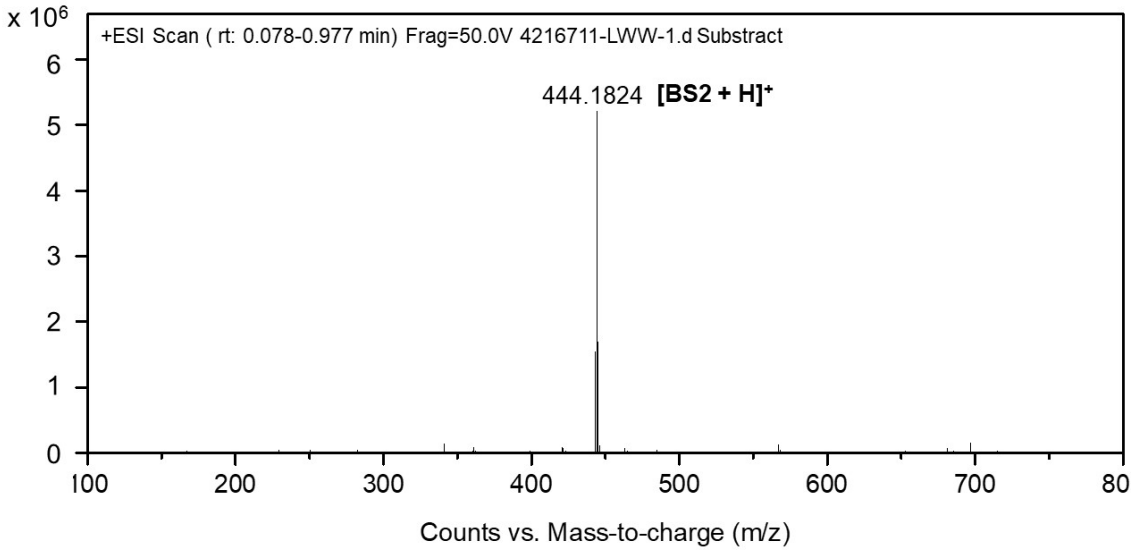

Fig. S7 ESI-high resolution mass spectra of probe **BS2**.

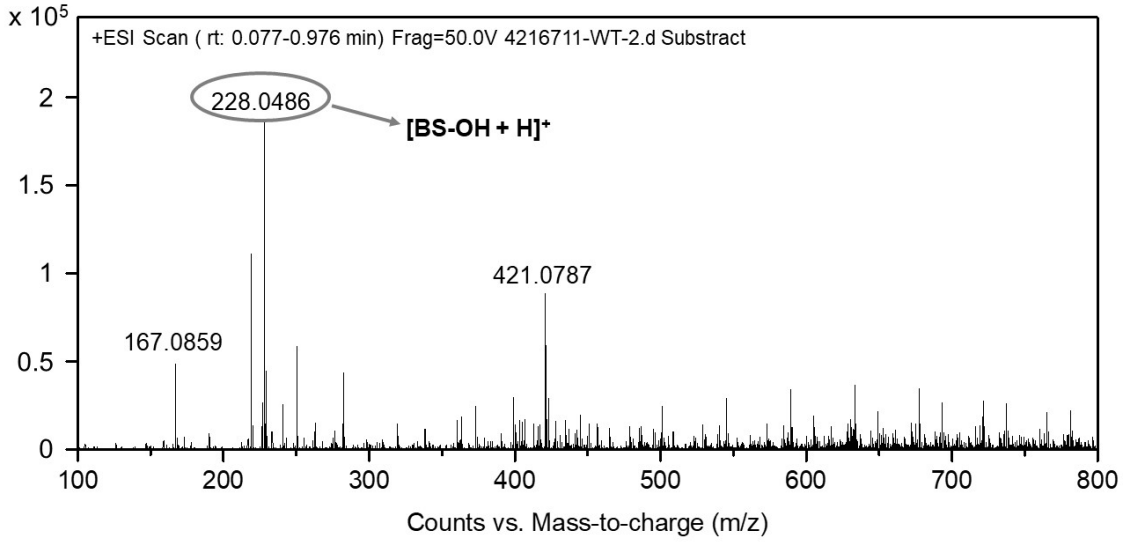

Fig. S8 ESI-high resolution mass spectra of **BS1** upon addition of $ONOO^-$.

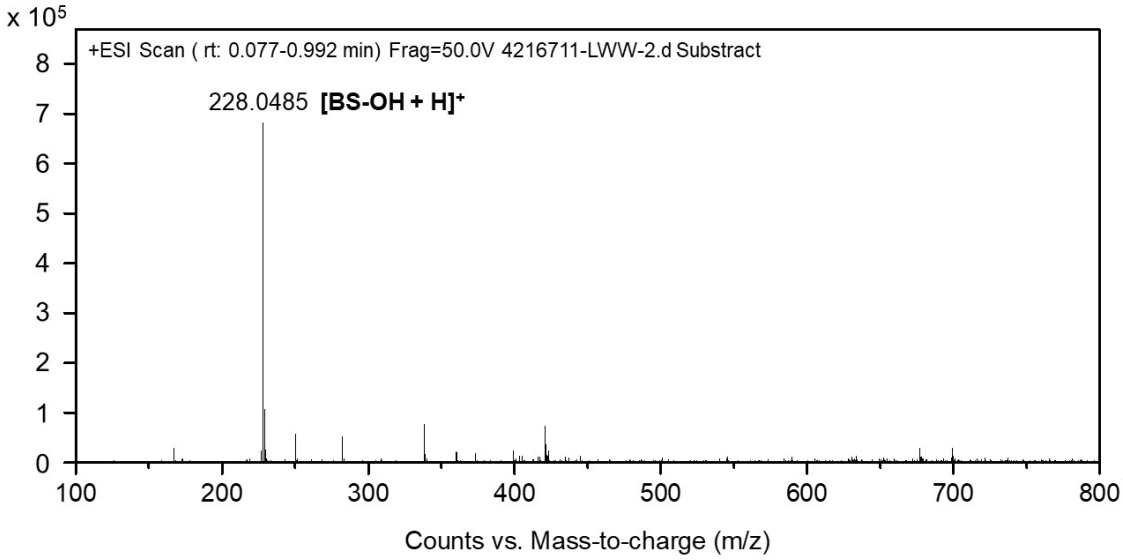

Fig. S9 ESI-high resolution mass spectra of **BS2** upon addition of $ONOO^-$.

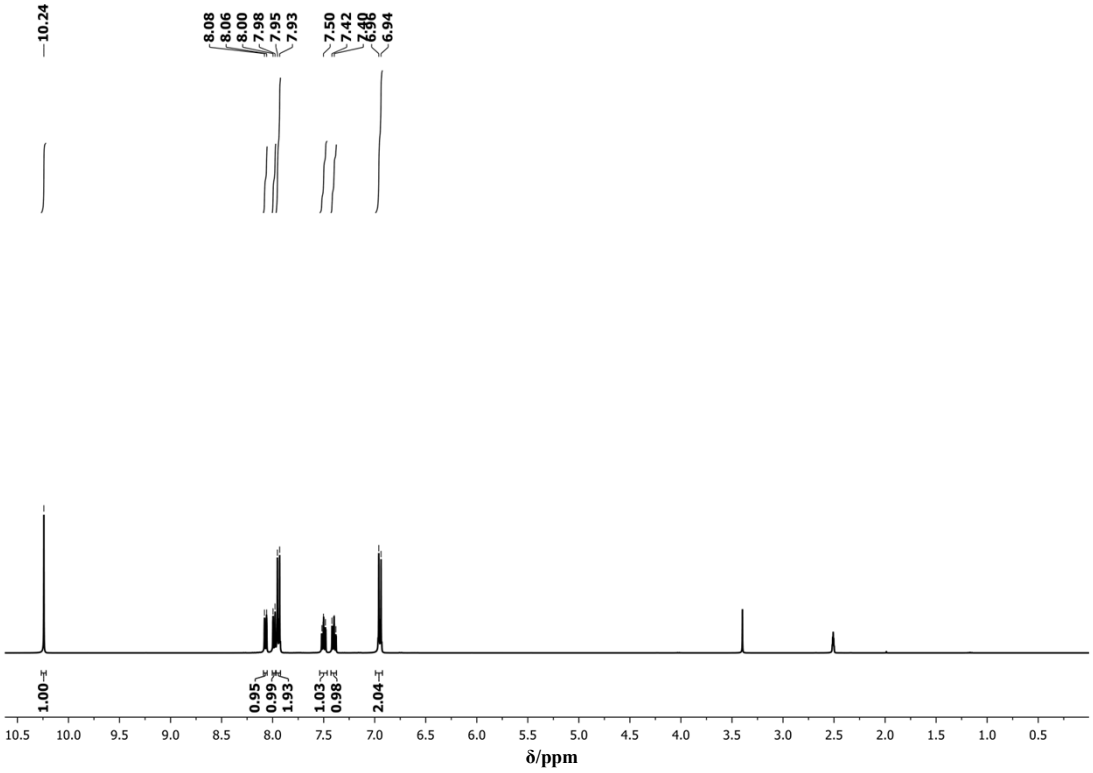

Fig. S10 The reaction product of ^1H NMR for **BS1** with $ONOO^-$ in d_6-DMSO.

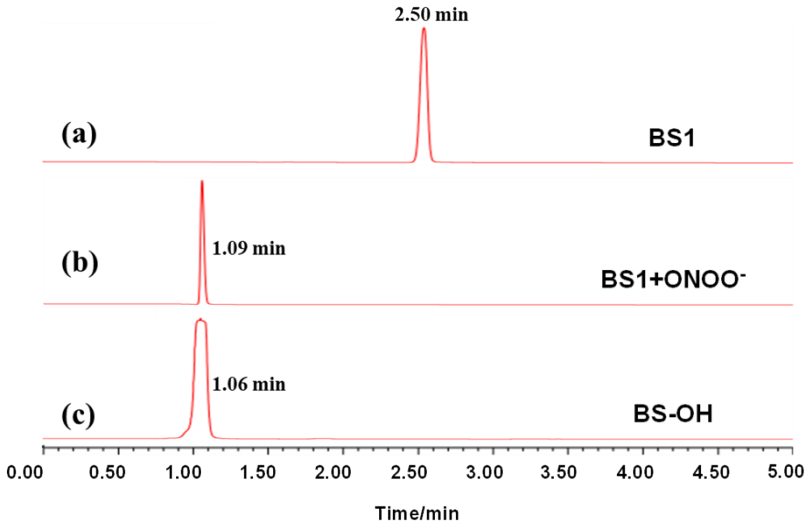

Fig. S11 The reverse-phase HPLC with absorption (254 nm) detection. (a) Probe **BS1**; (b) the reaction mixture of **BS1** and $ONOO^-$; (c) **BS-OH**.

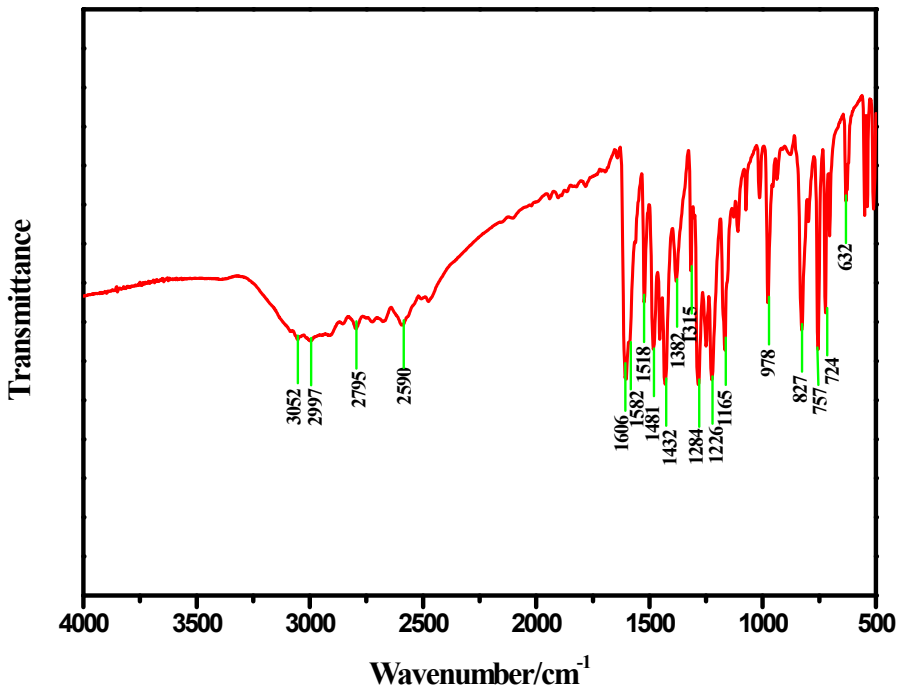

Fig. S12 The reaction product of FTIR spectrum for **BS2** with $ONOO^-$.

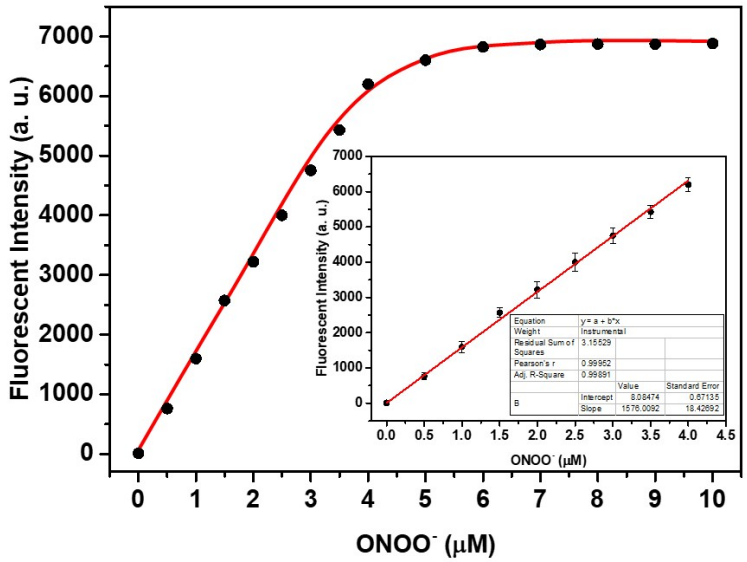

Fig. S13 Concentration-dependent intensity changes of **BS1** centered at 430 nm. The linear fitting of the plot of fluorescence intensity against $ONOO^-$ concentrations at 430 nm. λ_{ex} = 365 nm.

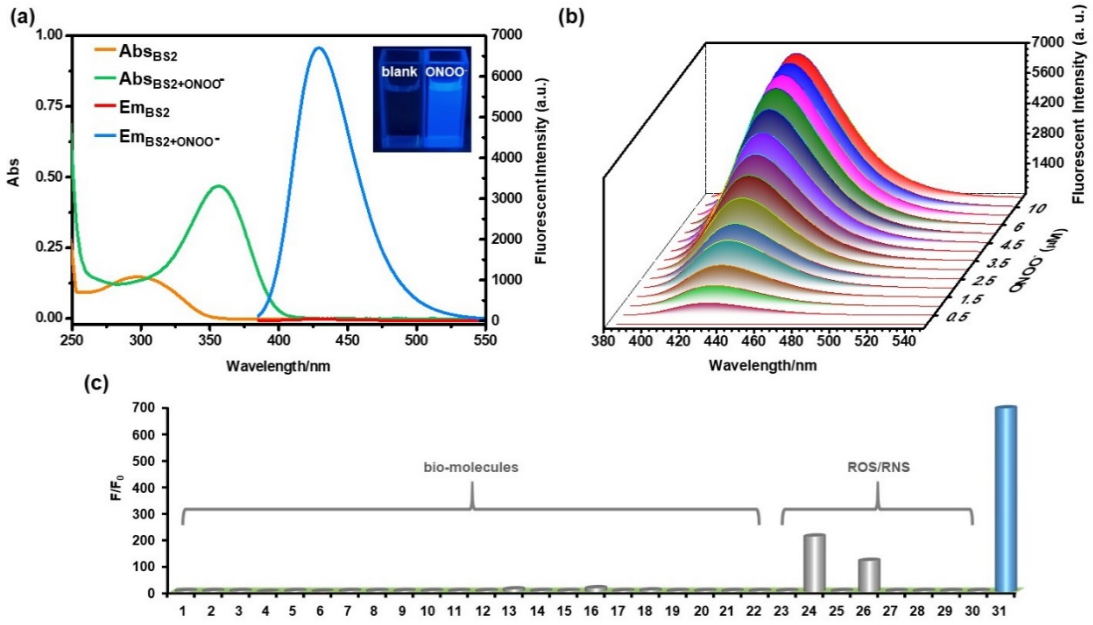

Fig. S14 (a) Absorption and fluorescence spectra of **BS2** before and after reacting with $ONOO^-$. Inset: photographs of reaction mixture in the absence (left) and presence (right) of $ONOO^-$ under 365 nm lamp. (b) Changes in fluorescence intensity of **BS2** (10 μM)

upon addition of different amounts of $ONOO^-$ (0-15 μM). (c) Fluorescence response of **BS2** (10 μM) at 430 nm with various bioanalytes: (1) blank; (2) Na^+ (1.0 mM); (3) K^+ (1.0 mM); (4) Fe^{3+} (1.0 mM); (5) Zn^{2+} (1.0 mM); (6) Cu^{2+} (1.0 mM); (7) Ca^{2+} (1.0 mM); (8) Al^{3+} (1.0 mM); (9) Mg^{2+} (1.0 mM); (10) SO_3^{2-} (1.0 mM); (11) SO_4^{2-} (1.0 mM); (12) CO_3^{2-} (1.0 mM); (13) HCO_3^- (1.0 mM); (14) NO_2^- (1.0 mM); (15) NO_3^- (1.0 mM); (16) PO_4^{3-} (1.0 mM); (17) Cl^- (1.0 mM); (18) H_2S (1.0 mM); (19) GSH (1.0 mM); (20) Cys (1.0 mM); (21) Vitamin C (1.0 mM); (22) AcOK (1.0 mM); (23) ·OH (1.0 mM); (24) H_2O_2 (0.5 mM); (25) $^1O_2$ (1.0 mM); (26) NaClO (0.5 mM); (27) NO (1.0 mM); (28) TBHP (1.0 mM); (29) HNO (1.0 mM); (30) $O_2^{\bullet -}$ (1.0 mM); (31) $ONOO^-$ (0.02 mM). All data were recorded in 10 mM PBS buffer (pH = 7.4) containing with 25% DMSO. λ_{ex}: 365 nm.

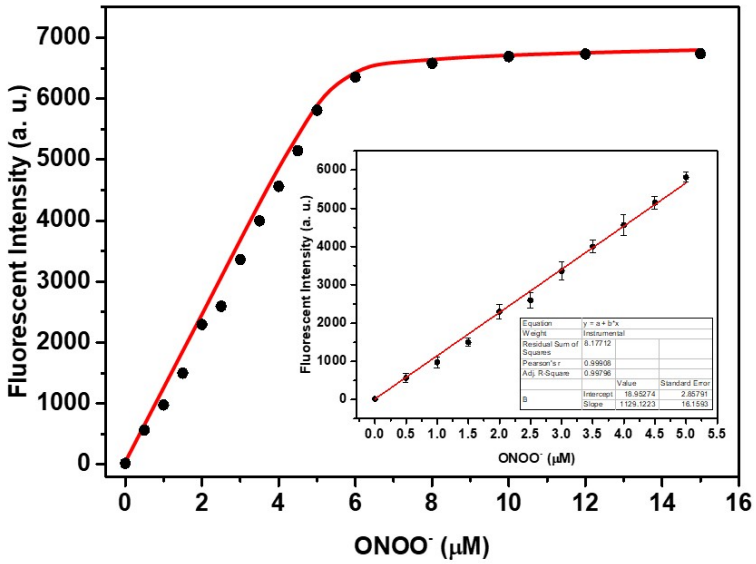

Fig. S15 Concentration-dependent intensity changes of **BS2** centered at 430 nm. The linear fitting of the plot of fluorescence intensity against $ONOO^-$ concentrations at 430 nm. λ_{ex} = 365 nm.

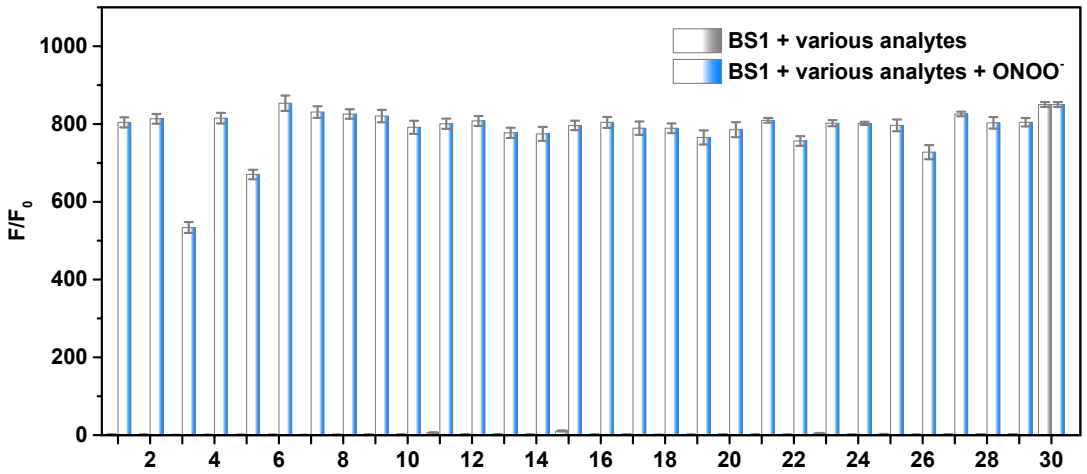

Fig. S16 Anti-interference study of **BS1** at 430 nm induced by $ONOO^-$ in the presence of various bioanalytes: (1) Na^+ (1.0 mM); (2) K^+ (1.0 mM); (3) Fe^{3+} (1.0 mM); (4) Zn^{2+} (1.0 mM); (5) Cu^{2+} (1.0 mM); (6) Ca^{2+} (1.0 mM); (7) Al^{3+} (1.0 mM); (8) Mg^{2+} (1.0 mM); (9) SO_3^{2-} (1.0 mM); (10) SO_4^{2-} (1.0 mM); (11) CO_3^{2-} (1.0 mM); (12) HCO_3^- (1.0 mM); (13) NO_2^- (1.0 mM); (14) NO_3^- (1.0 mM); (15) PO_4^{3-} (1.0 mM); (16) Cl^- (1.0 mM); (17) H_2S (1.0 mM); (18) GSH (1.0 mM); (19) Cys (1.0 mM); (20) Vitamin C (1.0 mM); (21) AcOK (1.0 mM); (22) ·OH (1.0 mM); (23) H_2O_2 (0.5 mM); (24) $^1O_2$ (1.0 mM); (25) NaClO (0.5 mM); (26) NO (1.0 mM); (27) TBHP (1.0 mM); (28) HNO (1.0 mM); (29) $O_2^{\bullet -}$ (1.0 mM); (30) $ONOO^-$ (0.01 mM). Gray column and blue column represent fluorescence response of **BS1** (10 μM) in the presence and absence of $ONOO^-$ (0.01 mM), respectively. λ_{ex} = 365 nm.

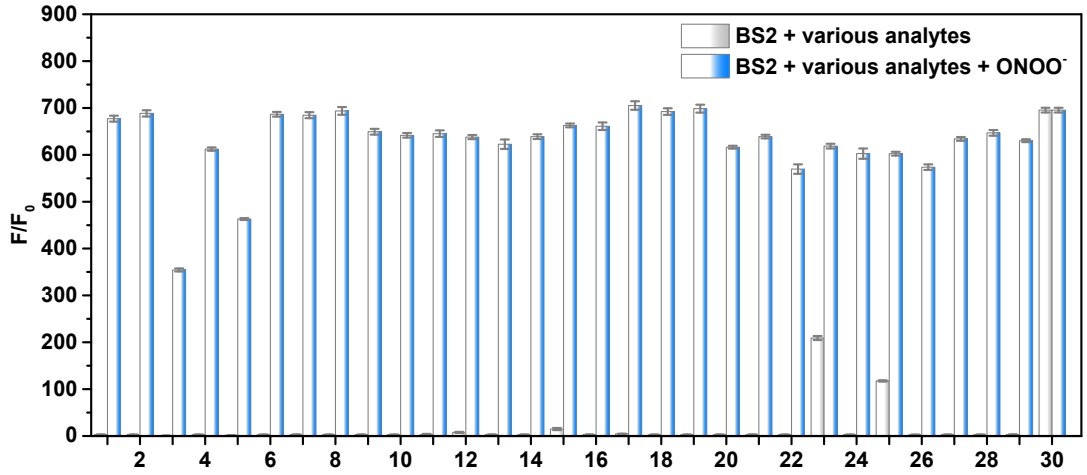

Fig. S17 Anti-interference study of **BS2** at 430 nm induced by $ONOO^-$ in the presence of various bioanalytes: (1) Na^+ (1.0 mM); (2) K^+ (1.0 mM); (3) Fe^{3+} (1.0 mM); (4) Zn^{2+} (1.0 mM); (5) Cu^{2+} (1.0 mM); (6) Ca^{2+} (1.0 mM); (7) Al^{3+} (1.0 mM); (8) Mg^{2+} (1.0 mM); (9) SO_3^{2-} (1.0 mM); (10) SO_4^{2-} (1.0 mM); (11) CO_3^{2-} (1.0 mM); (12) HCO_3^- (1.0 mM); (13) NO_2^- (1.0 mM); (14) NO_3^- (1.0 mM); (15) PO_4^{3-} (1.0 mM); (16) Cl^- (1.0 mM); (17) H_2S (1.0 mM); (18) GSH (1.0 mM); (19) Cys (1.0 mM); (20) Vitamin C (1.0 mM); (21) AcOK (1.0 mM); (22) ·OH (1.0 mM); (23) H_2O_2 (0.5 mM); (24) $^1O_2$ (1.0 mM); (25) NaClO (0.5 mM); (26) NO (1.0 mM); (27) TBHP (1.0 mM); (28) HNO (1.0 mM); (29) $O_2^{\bullet -}$ (1.0 mM); (30) $ONOO^-$ (0.02 mM). Gray column and blue column represent fluorescence response of **BS2** (10 μM) in the presence and absence of $ONOO^-$ (0.02 mM), respectively. λ_{ex} = 365 nm.

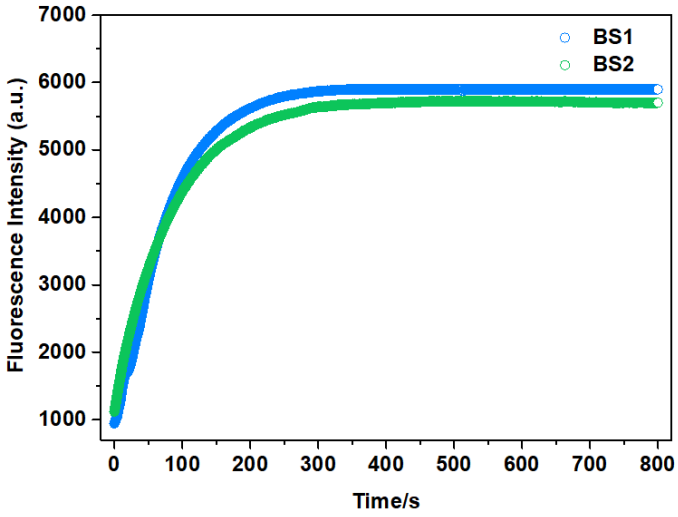

Fig. S18 Time-dependent intensity changes of **BS1** and **BS2** upon addition of $ONOO^-$ at 430 nm. λ_{ex} = 365 nm.

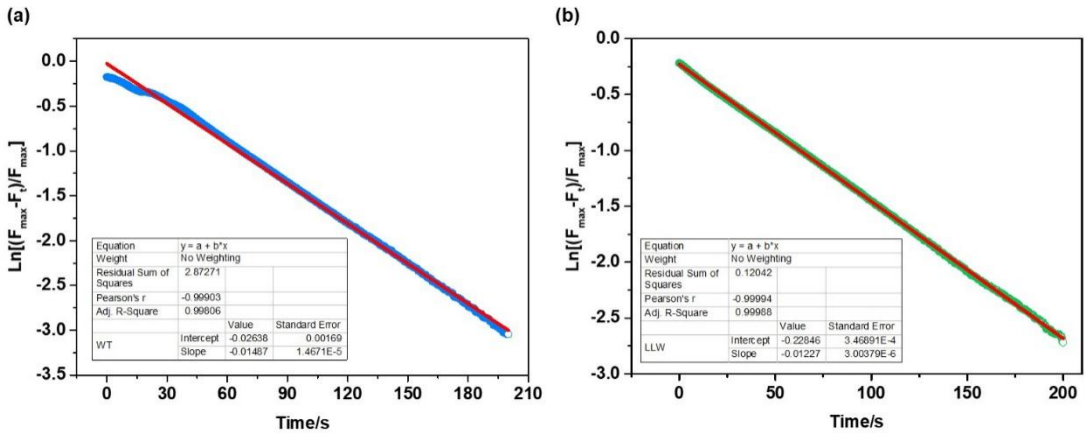

Fig. S19 Pseudo first-order kinetic plot of reaction of probe **BS1** and **BS2** with upon addition of $ONOO^-$.

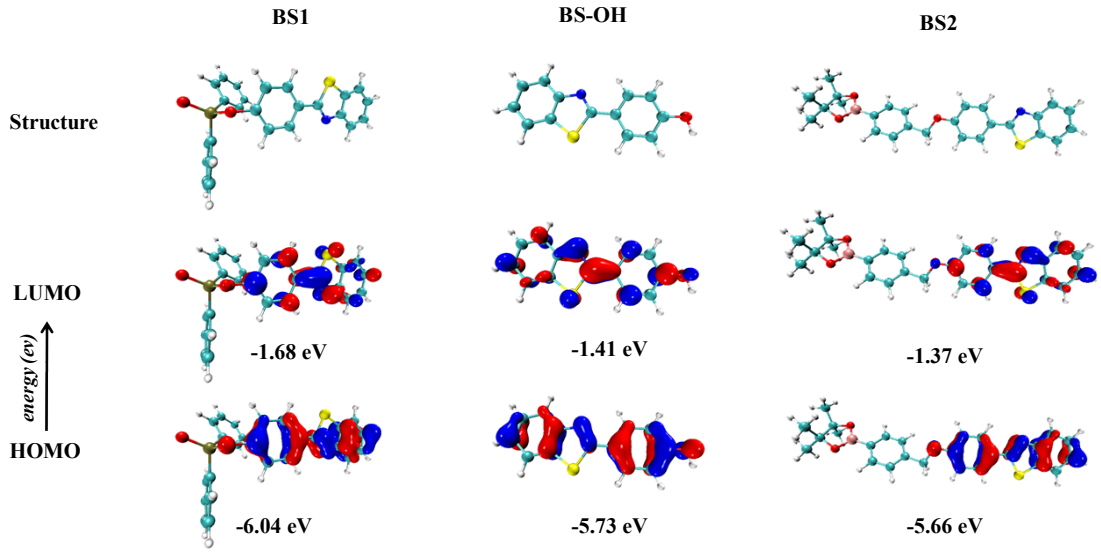

Fig. S20 The density functional theory (DFT) optimized structures and frontier molecular orbitals (MOs) of **BS1**, **BS2** and **BS-OH** at B3LYP/6-31G(d, p) level.

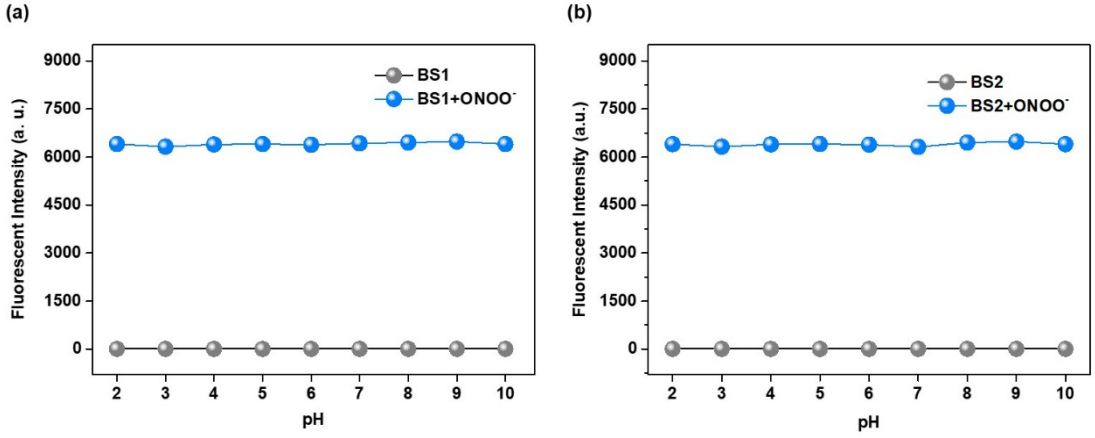

Fig. S21 The fluorescent change of **BS1** and **BS2** with (blue) or without (gray) $ONOO^-$ under different pH values at 430 nm. λ_{ex} = 365 nm.

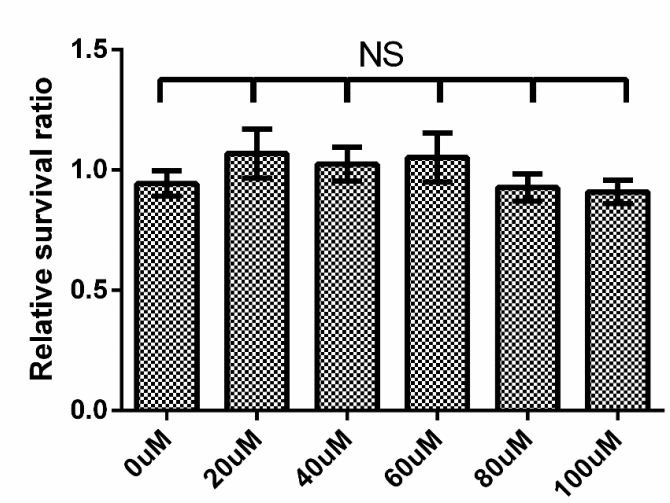

Fig. S22 CCK-8 assays of **BS1** at different concentrations (0, 20, 40, 60, 80, 100 μM) for HepG2 cells. NS: No signaficantly difference.

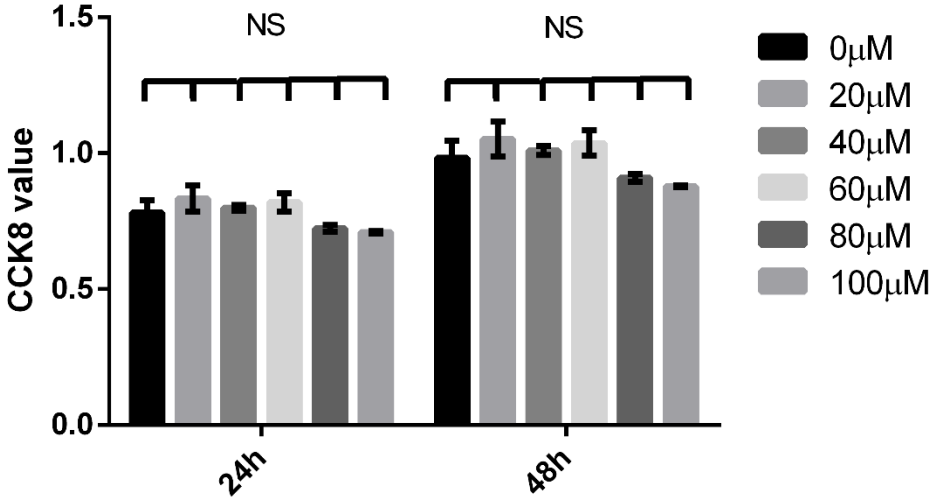

Fig. S23 CCK-8 value of **BS1** at different concentrations (0, 20, 40, 60, 80 and 100 μM) on HepG2 cells detected by CCK-8 for 48 h. NS not significant.

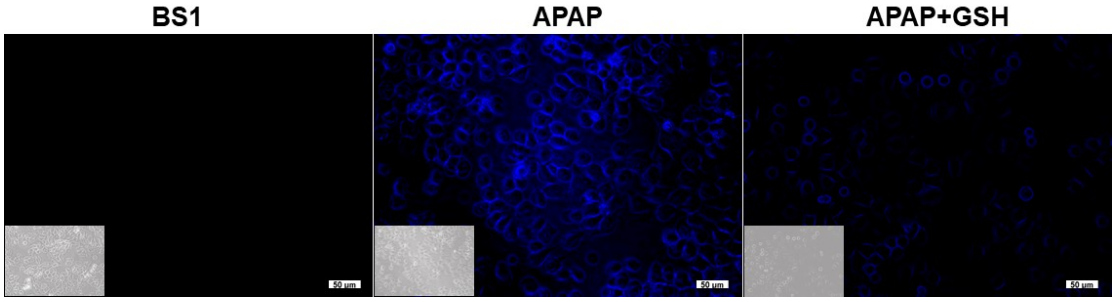

Fig. S24 Fluorescent imaging of remediation of APAP-induced hepatotoxicity with GSH in living HepG2 cells. (a) The cells were incubated with **BS1** (10 μM) for 30 min. (b) Cells were exposed to APAP (500 μM) for 8 h, and then incubated with **BS1** (10 μM) for 30 min. (c) Cells were pretreated with GSH (500 μM) for 1 h, and then incubated with APAP (500 μM) for 8 h, followed by incubated with **BS1** (10 μM) for 30 min. The images were obtain with 405 nm excitation and 420-490 nm collection. Scale bar: 50 μm.

References

[1] H. Li, J. Chao, Z. Zhang, G. Tian, J. Li, N. Chang and C. Qin, Org. Lett., 2020, **22**, 3323-3328.

[2] X. Han, X. Yang, Y. Zhang, Z. Li, W. Cao, D. Zhang and Y. Ye, Sens. Actuators B Chem., 2020, **321**, 128510.

[3] W. H. Melhuish, J. Phys. Chem. B, 1960, **65**, 229-235.

[4] R. Shen and Y. Qian, Dyes Pigments, 2020, **176**, 108247.

[5] Y. Li, X. Xie, X. Yang, M. Li, X. Jiao, Y. Sun, X. Wang and B. Tang, Chem. Sci., 2017, **8**, 4006-4011.

[6] P. J. Ogren, A. Meetze and W. C. Duer, J. Anal. Toxicol., 2009, **33**, 129-142.

[7] M. J. Frisch, G. W. Trucks, H. B. Schlegel, et al. Gaussian 16 rev. C.01, edited, Wallingford, CT, 2016.

[8] T. Lu and F. Chen. J. Comput. Chem., 2012, **33**, 580-592.

[9] W. Humphrey, A. Dalke and K. Schulten. J. Mol. Graph., 1996, **14**, 33-38.

[10] Y. Fu, H. Nie, R. Zhang, F. Xin, Y. Tian, J. Jing and X. Zhang, RSC Adv., 2018, **8**, 1826-1832.

[11] D. Wu, J. C. Ryu, Y. W. Chung, D. Lee, J. H. Ryu, J. H. Yoon and J. Yoon, Anal. Chem., 2017, **89**, 10924-10931.

[12] Y. Guo, G. Lu, J. Zhuo, J. Wang, X. Li and Z. Zhang, J. Mater. Chem. B, 2018, **6**, 2489-2496.

[13] Y. Wu, A. Shi, Y. Li, H. Zeng, X. Chen, J. Wu and X. Fan, Analyst, 2018, **143**, 5512-5519.

[14] X. Sun, K. Lacina, E. C. Ramsamy, S. E. Flower, J. S. Fossey, X. Qian, E. V. Anslyn, S. D. Bull and T. D. James, Chem. Sci., 2015, **6**, 2963-2967.

[15] J. Li, S. L. Chang, G. Kim, H. M. Kim and J. Yoon, Anal. Chem., 2017, **89**, 8496-8500.

[16] J. Kim, J. Park, H. Lee, Y. Choi and Y. Kim, Chem. Commun., 2014, **50**, 9353-9356

[17] Y. Shen, X. Zhang, Y. Zhang, H. Li, L. Dai, X. Peng, Z. Peng and Y. Xie, Anal. Chim. Acta, 2018, **1014**, 71-76.

[18] S. Palanisamy, P. Y. Wu, S. C. Wu, Y. J. Chen, S. C. Tzou, C. H. Wang, C. Y. Chen and Y. M. Wang, Biosens. Bioelectron., 2017, **91**, 849-856.

[19] X. Zhou, Y. Kwon, G. Kim, J. H. Ryu and J. Yoon, Biosens. Bioelectron., 2015, **64**, 285-291.